RSC Advances

PAPER

View Article Online
View Journal | View Issue

Cite this: *RSC Adv.*, 2017, **7**, 50961

Tunable laser operations in a Nd-doped $SrLaAlO_4$ crystal

Lulu Dong,[ab] Yan Xu,[ab] Yongping Yao,[b] Qiangguo Wang,[b] Shande Liu,[*b] Tingqi Ren,[*b] Lihe Zheng,[*c] Liangbi Su,[c] Yandong Peng[b] and Marek Berkowski[d]

Received 16th August 2017
Accepted 6th October 2017

DOI: 10.1039/c7ra09058g

rsc.li/rsc-advances

Tunable laser operations in a disordered crystal, Nd:$SrLaAlO_4$, were experimentally reported. The maximum tuning range of 32 nm from 1063 to 1095 nm was achieved with a birefringent filter (Lyot filter). The maximum output power was 1.66 W at the center wavelength of 1075.5 nm, giving an optical-to-optical efficiency of 30%. The output power over 50% of the tuning range was greater than 0.6 W. The special spectral lines, such as 1073, 1080 and 1083 nm, have a potential application in the field of atom and molecular spectroscopy.

1. Introduction

Over past and present years, materials research for tunable lasers has attracted a lot of attention. They constitute a system of high interest in a great variety of fields, such as remote environmental sensing, optical networks, spectroscopy and frequency conversion, where a tunable and narrow spectral line is needed.[1] Ytterbium (Yb) doped materials are regarded as a promising kind of gain media for 1 μm solid-state lasers, due to the strong electron-phonon coupling of Yb-ions resulting in significant spectrum broadening.[2,3] Great efforts have been made in the past few years to generate widely tunable Yb-doped lasers and some encouraging results have been achieved. In 2007 V. Petrov *et al.* reported highly efficient Yb:$NaY(WO_4)_2$ tunable lasers, with a tunability range of 69 nm.[4] After that, J. Xu *et al.* presented widely tunable Yb-doped silicate lasers.[5,6] However, the limit of the reported tuning range from the Yb-doped crystal was shorter than 1080 nm. Besides, the overlapping of emission and absorption bands leads to additional re-absorption loss, resulting in a high lasing threshold. Compared with the Yb^{3+}-doped materials, Nd^{3+}-doped materials have negligible re-absorption loss and a large emission cross section, thus they have been widely applied in high-power laser oscillators and amplifiers.[7,8] Nevertheless, most of the homogeneous Nd^{3+}-doped tunable lasers could normally generate a small tuning range as a result of the narrow gain bandwidth (such as Nd:YVO_4, 0.96 nm and Nd:YAG, 0.8 nm). Nd^{3+}:glass emerged as another Nd-doped gain medium, and possesses a very broad gain bandwidth and has been realized for tunable laser operation with a tuning coverage of 12 nm.[9] However, its intrinsic poor thermal property makes it difficult to generate high-power and high repetition rate laser pulses.

Different from the Nd^{3+}:glass, Nd^{3+}-doped disordered crystals not only possess broad absorption and gain bandwidth, but also have extraordinary thermal properties. Such characteristics make them suitable candidates for generating a high-power tunable laser. To date, several Nd^{3+}-doped disordered crystals, such as Nd:SBN,[10] Nd, La:SrF_2 (ref. 11) and Nd:YAP,[12] have been realized for tunable laser operations. In addition, the Nd:$SrLaAlO_4$ (Nd:SLA) crystal, first grown by the M. Berkowski group, is also a promising disordered crystal with a tetragonal K_2NiF_4 structure. In this structure, the Sr and La atoms are distributed randomly in the symmetrical sites resulting in larger ground-state splitting and broad emission spectra, which is suitable for ultrafast and tunable laser operations. It can be clearly seen that there are various attainable emission peaks in the range of 1050 to 1100 nm.[13] The transition lines at 1073, 1080 and 1083 nm especially have proven to be useful for the optical pumping of superfluid helium and related scientific applications such as molecular spectroscopy.[14,15] A lot of research has been done to demonstrate the spectral characteristics. For example, a 458 fs stable mode-locked Nd:SLA laser was first realized by S. D. Liu *et al.*[16] with an output power of 0.52 W. Unfortunately, there is no research on this Nd:SLA tunable laser. Therefore, it is significant to study the tunable properties of the Nd:SLA crystal and to further reveal a potential application in the field of atom and molecular spectroscopy.

[a]*College of Electrical, Engineering and Automation, Shandong University of Science and Technology, Qingdao 266590, China*

[b]*College of Electronic, Communication and Physics, Shandong University of Science and Technology, Qingdao 266590, China. E-mail: pepsl_liu@163.com; rentingqi@163.com*

[c]*Key Laboratory of Transparent and Opto-functional Inorganic Materials, Shanghai Institute of Ceramics, Chinese Academy of Science, Shanghai 200050, China. E-mail: zhenglihe@gmail.com*

[d]*Institute of Physics, Polish Academy of Science, Al. Lotników, 32/46, 02-668 Warsaw, Poland*

2. Experimental setup

The tunable laser was realized in a V-type cavity, as schematically shown in Fig. 1. The pump source was a fiber-coupled LD operating at 808 nm with a numerical aperture of 0.22. The laser beam was collimated into the gain medium with a spot waist radius of 200 μm by a 1 : 1 coupling optics system. A 3 mm-long Nd:$SrLaAlO_4$ crystal with a neodymium concentration of 1% was applied as the gain medium, with a cross section of 2×2 mm^2. The crystal was uncoated. To remove accumulated heat, the crystal was wrapped with indium foil and tightly mounted in a copper block cooled by water at a temperature of 18 °C. The flat mirror M_1 ($R = \infty$) and concave mirror M_2 ($R = 200$ mm) were employed as the input and folded mirror, respectively; both of which were AR coated at 808 nm and HR coated with a broad band from 1–1.1 μm. M_3 was a flat output mirror with different transmissions of 5%, 10% and 25% at 1–1.1 μm. The distances between M_1, M_2 and M_3 were 220 and 175 mm, respectively. The folded angle of mirror M_2 in the V-type cavity was as small as possible to decrease the astigmatism between the oscillation modes of sagittal and tangential directions. A 2 mm-thick quartz birefringent filter (BF) was applied as a wavelength selective device. The average output power and spectra were measured with a laser power meter (Fieldmax-II, Coherent) and an optical analyzer (Avantes, AcaSpec-3648-NIR256-2.2), respectively.

3. Results and discussions

By fine tuning the pitch angle of the crystal and cavity mirrors, a continuous-wave Nd:SLA laser was firstly realized. The CW output power *versus* the absorbed pump power is shown in Fig. 2. Due to the relatively high absorption coefficient and reasonable crystal quality, the absorption efficiency of this crystal at the pump wavelength was measured to be 93%. As can be seen from Fig. 2, the lasing threshold pump powers were 0.09, 0.25 and 1.04 W with output couplers of $T_{oc} = 3\%$, 10% and 25%, respectively. Based on the model developed by Findlay and Clay[17] the threshold pump power can be given by $P_{th} = K(\delta + T)$, where K is a constant for the crystal and cavity, T is the transmission of the output couplers and δ is the round-trip loss mainly induced by the absorption, scattering and non-uniformity of the laser crystal. With $P_{th} = 0.09$ W, $T = 0.03$ and $P_{th} = 0.25$ W, $T = 0.1$, the parameter δ was calculated to be 0.009, which revealed that the Nd:SLA crystal was of reasonable quality. With an output coupler of $T_{oc} = 10\%$, a maximum output power was obtained to be 2.51 W under an absorbed pump power of 5.58 W, corresponding to an optical-to-optical efficiency of 45% and a slope efficiency of 48%.

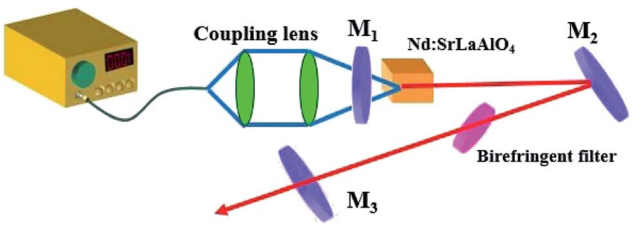

Fig. 1 Cavity configuration of the tunable Nd:SLA laser.

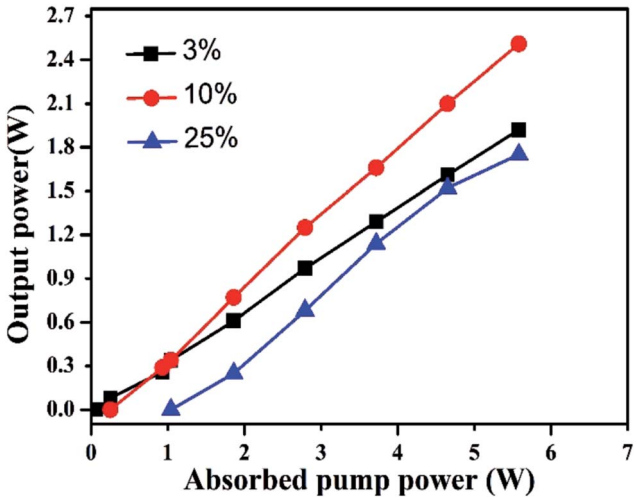

Fig. 2 The relationship between CW output power and absorbed pump power.

The tuning of laser radiation was accomplished by inserting a quartz BF oriented at Brewster's angle in the M_2–M_3 arm close to the output coupler. At optimum alignment, the output power with the filter inside the cavity was recorded and is shown in Fig. 3. With an output coupler of $T = 3\%$, a maximum output power of 1.49 W was achieved under an absorbed pump power of 5.58 W. The proportion of with and without filter was about 77%. It is worthwhile to mention that the reduction in output power can be attributed to the degree of polarization and additional intracavity loss of the quartz BF.

The schematic of the quartz birefringent filter is shown in Fig. 4. For that, the transmitted intensity T can be expressed as:[18]

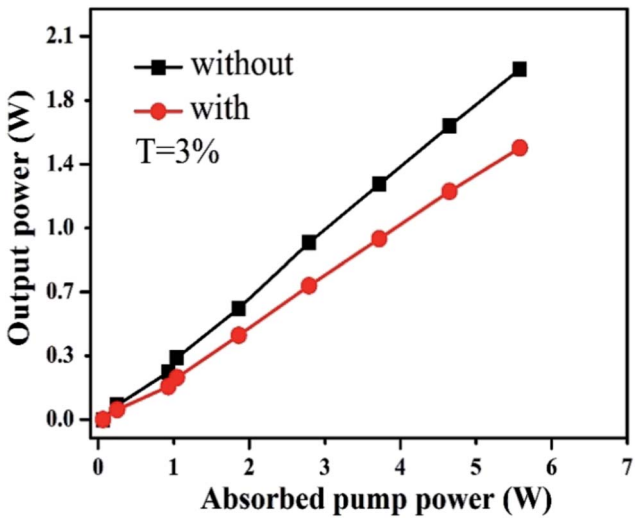

Fig. 3 The comparison of output power with (red dots) and without (black dots) the quartz BF in the laser cavity.

$$T = 1 - 4c\tan^2\gamma\tan^2\theta_b(1 - c\tan^2\gamma\tan^2\theta_b)\sin^2\frac{\Delta\varphi}{2} \quad (1)$$

$$\Delta\varphi = \frac{2\pi(n_0 - n_e)l}{\lambda\sin\theta_b}\sin^2\gamma \quad (2)$$

$$\cos^2\theta_b\cos^2\varphi = 1 - \sin^2\gamma \quad (3)$$

where γ is the angle between the optical axis and the refracted ray, θ_b is Brewster's angle, φ is the angle between the projection of the incident ray and the optical axis, $\Delta\varphi$ is the optical phase difference, λ is the wavelength and l is the length of the quartz crystal. When $\Delta\varphi = 2m\pi$ and $m = 0, \pm1, \pm2, \ldots$, the maximum transmitted intensity can be obtained, and the corresponding transmitted wavelength λ can be presented as:

$$\lambda = \frac{(n_0 - n_e)l}{m\sin\theta_b}\sin^2\gamma = C_0(1 - \cos^2\theta_b\cos^2\phi) \quad (4)$$

where n_0 and n_e are the refractive indexes of the ordinary and extraordinary light, respectively. For the given quartz BF, C_0 is a constant. The laser wavelength will be tunable with the change of the angle ϕ.

The tunable laser properties were investigated by carefully rotating the quartz BF. The tuning curve obtained for $T = 3\%$ is shown in Fig. 4. The absorbed pump power, fixed at 808 nm, was around 5.58 W. As shown, a continuous tuning range of 32 nm from 1063 to 1095 nm was achieved under our diode pump conditions and a maximum output power of 1.49 W was obtained at 1077.5 nm. The widely tunable coverage benefits from the emission spectrum property of inhomogeneous broadening. The output power was greater than 0.6 W over 50% tuning coverage. It is important to remark that almost the same tuning range was achieved for the absorbed pump powers close to the threshold value due to the four-level laser operation scheme of the Nd^{3+} ion. This is an advantage over tunable Yb^{3+} doped laser crystals with tuning range in the same spectral region, which require a higher pump power to realize similar tuning ranges due to their quasi-three energy level structure. Fig. 5 presents as an example several spectra recorded for the Nd:SLA tunable laser. The shortest and longest spectral lines for the Nd:SLA tunable laser are 1063 and 1095 nm, respectively.

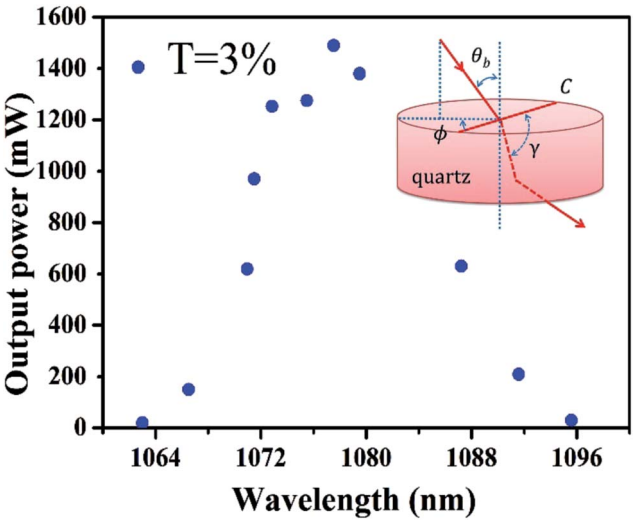

Fig. 4 Output power *versus* laser wavelength with $T = 3\%$ output coupler (inset: the schematic of the quartz BF).

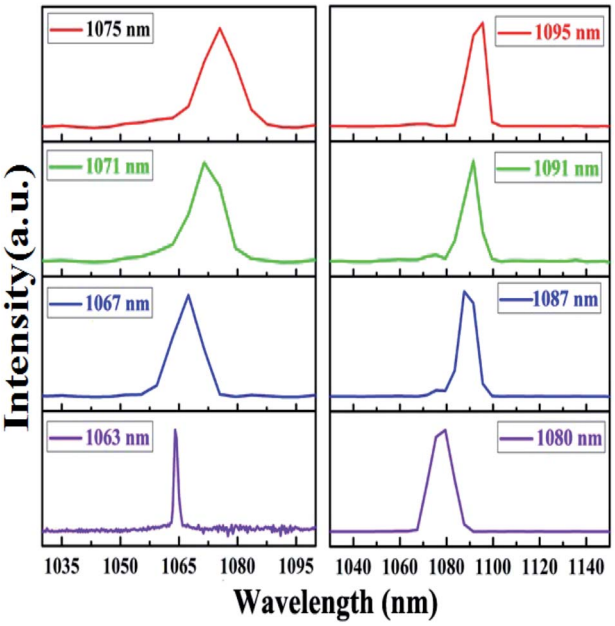

Fig. 5 Laser spectra for the Nd:SLA tunable laser.

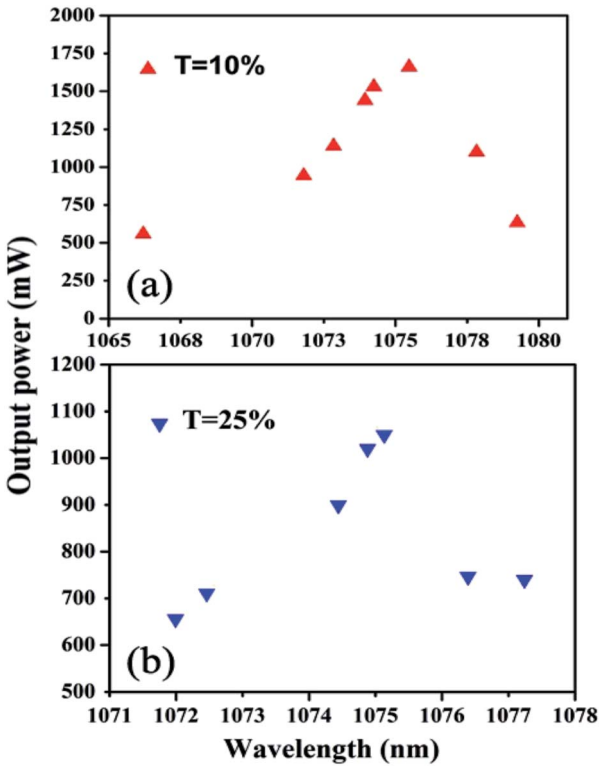

Fig. 6 Output power *versus* laser wavelength with $T = 10\%$ and $T = 25\%$ output coupler.

With an output coupler of $T = 10\%$ and 25%, the tunable characteristics were also investigated, as shown in Fig. 6. The tuning range was 13 nm with the $T = 10\%$ output coupler and the maximum output power was 1.66 W at 1075.5 nm. Over the whole tuning range, the laser output powers were still above 0.5 W. Compared with the $T = 3\%$ output coupler, the tunable laser possessed a higher output power and smaller tuning range. This can be attributed to the gain competition of different frequencies. By selecting $T = 25\%$ as an output coupler, the tuning range was further narrowed, but the output power was increased.

Finally, adjusting the angle of the BF to certain values for balancing the gain and loss can further allow our Nd:SLA laser to be operated in multi-wavelength states. Fig. 7(a)–(c) show the output spectra of the experimentally obtained multi-wavelength groups. The maximum output powers are found to be 1.22, 0.19 and 0.85 W for the multi-wavelength groups of (1073, 1080 and 1091 nm), (1065, 1073 and 1094 nm) and (1073 and 1094 nm), respectively. The dual-wavelength and tri-wavelength laser operations made the Nd:SLA crystal suitable for application in THz generation.[20] Due to the strong gain competition among different spectral emissions, the multi-wavelength operations became unstable when the output powers were beyond the maximum values.

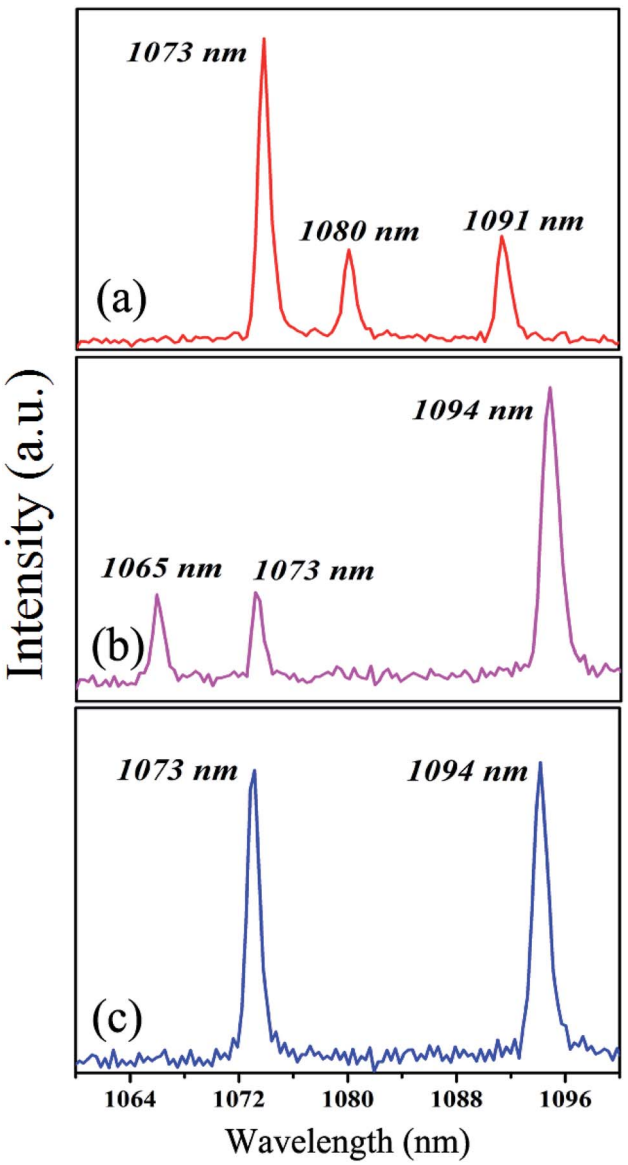

Fig. 7 Output spectra of the multi-wavelength Nd:SLA laser. (a) 1073, 1080 and 1091 nm. (b) 1065, 1073 and 1094 nm. (c) 1073 and 1094 nm.

Table 1 Comparisons of tuning range and output power for tunable Nd-doped lasers such as Nd:SBN, Nd:glass, Nd, La:SrF_2, Nd:BLG and Nd:SLA

Materials	Tuning range (nm)	Wavelength (nm)	Tuning element	Power (mW)
Nd:SBN[10]	43	1050–1093	BF	27
Nd:glass[9]	14	1057–1071	Etalon	3
Nd, La:SrF_2 (ref. 12)	24	1047–1071	Prism	320
Nd:BLG[19]	20	1070–1090	Prism	300
Nd:$SrLaAlO_4$ (this work)	**32**	**1063–1095**	**BF**	**1660**

To give a direct comparison, Table 1 lists primary tunable laser properties for some Nd-doped disordered materials. It can be seen that the maximum tuning range of 43 nm was obtained with the Nd:SBN crystal, however, the laser output power was only 27 mW. The superiority of the Nd:SLA tunable laser was that it possessed a high output power and wide tuning range simultaneously. Our experimental results indicated that the Nd:SLA crystal was a promising candidate for achieving an ultrafast laser and a highly efficient tunable laser.

4. Conclusions

In conclusion, we have experimentally demonstrated a diode-pumped Nd:SLA tunable laser. The tunability with different output couplers was fully investigated, and the results showed that a wide tuning range was easily achieved with an output coupler possessing a relatively lower transmittance. Taking advantage of the broad bandwidth gain, a 32 nm tuning range from 1063 to 1095 nm was obtained with a birefringent filter. With an output coupler of $T = 10\%$, the maximum output power was 1.66 W at the center wavelength of 1075.5 nm, giving an optical-to-optical efficiency of 30%. The output power over 50% of the tuning range was greater than 0.6 W. The special spectral lines, such as 1073, 1080 and 1083 nm, have a potential application in the field of atom and molecular spectroscopy.

Conflicts of interest

There are no conflicts to declare.

Acknowledgements

The authors would like to acknowledge funding support from the NSFC programs (61505098, 11547037, 61475177, 61775123), the NSAF program (U1530152), the SDUST Research Fund

(2015RCJJ013, 2015JQJH103, 2014JQJH104), the Postdoctoral Science Foundation of China (2015M572062), the Qingdao Postdoctoral Applied Research Project (No. 2015178), the Key Laboratory of Functional Crystal Materials and Device (JG1502) and the Major Fundamental Research of Shandong Province, China (ZR2017ZB0318).

Notes and references

1 M. Kues, C. Reimer, B. Wetzel, P. Roztockim, B. E. Little, S. T. Chu, T. Hansson, E. A. Viktorov, D. J. Moss and R. Morandotti, *Nat. Photonics*, 2017, **11**, 159–162.
2 Z. Y. Gao, J. F. Zhu, J. L. Wang, Z. Y. Wei, X. D. Xu, L. H. Zheng, L. B. Su and J. Xu, *Photonics Res.*, 2015, **3**, 335–338.
3 Q. Q. Hu, Z. T. Jia, A. Volpi, S. Veronesi, M. Tonelli and X. T. Tao, *CrystEngComm*, 2017, **19**, 1643–1647.
4 A. García-Cortés, J. M. Cano-Torrés, M. D. Serrano, C. Cascales, C. Zaldo, S. Rivier, X. Mateos, U. Griebner and V. Petrov, *IEEE J. Quantum Electron.*, 2007, **43**, 758–764.
5 J. P. He, X. Y. Liang, L. H. Zheng, L. B. Su, J. Xu and Z. Z. Xu, *Chin. Opt. Lett.*, 2009, **7**, 1028–1030.
6 H. Y. Zhang, J. F. Li, X. Y. Liang, H. Lin, L. H. Zheng, L. B. Su and J. Xu, *Chin. Opt. Lett.*, 2012, **10**, 111404.
7 M. Louis, W. Richard and N. Achim, *Opt. Lett.*, 2007, **32**, 1259–1261.
8 L. H. Zheng, A. Kausas and T. Taira, *Opt. Express*, 2016, **24**, 28748–28760.
9 Z. W. Fan, J. S. Qiu, Z. J. Kang, Y. Z. Chen, W. Q. Ge and X. X. Tang, *Light: Sci. Appl.*, 2017, **6**, 17004.
10 M. O. Ramírez, J. J. Romero, P. Molina and L. E. Bausa, *Appl. Phys. B*, 2005, **81**, 827–830.
11 F. Zhang, H. N. Zhang, D. H. Liu, J. Liu, F. K. Ma, D. P. Jiang, S. Y. Pang, L. B. Su and J. Xu, *Chin. Phys. B*, 2017, **26**, 024205.
12 Y. S. Tzeng, Y. J. Huang, C. Y. Tang, K. W. Su, W. D. Chen, G. Zhang and Y. F. Chen, *Opt. Express*, 2013, **21**, 26261–26268.
13 S. D. Liu, L. L. Dong, X. Zhang, Y. P. Yao, Y. Xu, T. Q. Ren, L. H. Zheng, L. B. Su and M. Berkowski, *Opt. Mater.*, 2017, **64**, 351–355.
14 L. D. Schearer and P. Tin, *J. Appl. Phys.*, 1990, **68**, 943–949.
15 P. C. Rellergert, S. B. Cahn, P. De Natale, G. Hagel, C. De Mauro and M. Inguscio, *Phys. Rev. Lett.*, 2014, **92**, 023001.
16 S. D. Liu, L. L. Dong, L. H. Zheng, M. Berkowski, L. B. Su, T. Q. Ren, Y. D. Peng, J. Hou, B. T. Zhang and J. L. He, *Appl. Phys. Express*, 2016, **9**, 072701.
17 D. Findlay and R. A. Clay, *Phys. Lett.*, 1966, **20**, 277–278.
18 S. M. Kobtsev and N. A. Sventsitskaya, *Opt. Spectrosc.*, 1992, **73**, 114–123.
19 A. Agnesi, F. Pirzio, L. Tartara, E. Ugolotti, H. Zhang, J. Wang, H. Yu and V. Petrov, *Laser Phys. Lett.*, 2014, **11**, 035802.
20 G. Q. Xie, D. Y. Tang, H. Luo, H. J. Zhang, H. H. Yu, J. Y. Wang, X. T. Tao, M. H. Jiang and L. J. Qian, *Opt. Lett.*, 2008, **33**, 1872.